

Article

Highly Active Catalysts for the Dehydration of Isopropanol

Martyna Murat ^{*}, Zdeněk Tišler , Josef Šimek and José M. Hidalgo-Herrador 

Unipetrol Výzkumně Vzdělávací Centrum, a.s., 400 01 Ústí nad Labem, Revoluční 1521/84, Czech Republic; zdenek.tisler@unicre.cz (Z.T.); josef.simek@unicre.cz (J.Š.); jose.hidalgo@unicre.cz (J.M.H.-H.)

* Correspondence: martyna.murat@unicre.cz; Tel.: +420-471-122-235

Received: 28 May 2020; Accepted: 24 June 2020; Published: 26 June 2020



Abstract: Due to the high costs and low selectivity associated with the production of propylene, new routes for its synthesis are being sought. Dehydration has been widely investigated in this field, but, thus far, no study has produced efficient results for isopropanol. Vanadium-zirconia catalysts have been shown to be effective for the dehydration of ethanol. Therefore, we investigated the activity of such catalysts in the dehydration of isopropanol. The catalysts were synthesized on a SBA-15 base, supplemented with zirconia or combined zirconia and vanadium. Tests were conducted in a continuous flow reactor at 150–300 °C. Samples were analyzed using a gas chromatograph. The most active catalyst showed 96% conversion with 100% selectivity to propylene. XRD, SEM and Raman spectroscopy analyses revealed that as the vanadium content increases, the pore size of the catalyst decreases and both isopropanol conversion and propylene selectivity are reduced. Thus, without the addition of vanadium, the Zr-SBA-15 catalyst appears to be suitable for the dehydration of isopropanol to propylene.

Keywords: isopropanol; propylene; dehydration; catalysis; SBA-15; vanadium; zirconia

1. Introduction

Propylene is the second most-used raw material in plastics processing and the global demand for it is expected to reach 140 MMT in 2020 [1]. It is utilized in the production of chemicals with a wide range of applications, including polypropylene, phenol, propylene glycol and aldehydes. The biggest producers of propylene are refineries, where it is produced by the steam cracking or fluid catalytic cracking (FCC) of higher hydrocarbons [2]. However, these processes are dependent on crude oil, are costly and produce propylene with low selectivity. Consequently, researchers are looking for ways of obtaining good yields of highly selective propylene at a lower cost and with green chemistry being a hot and necessary topic, in an environmentally friendly way.

With green chemistry being necessary and very popular nowadays, isopropyl alcohol that can be produced by bacteria is considered a good potential precursor for propylene production by selective dehydration [3]. Unfortunately, there has been no satisfying research in this field [4].

The dehydration of isopropanol presents several environmental and strategic advantages over classical steam cracking. The development of cost-effective, environmentally friendly propanol fermentation processes, which are now being developed, may not only satisfy the direct demand for isopropanol but also its production as a precursor of propylene [2,5].

Products from dehydration depend on the given reaction conditions and chosen catalyst, which in this particular case, are the metal particle size and composition of the carrier [6]. Specifically, supported vanadium-based catalysts have been found to be active in promoting the dehydration of ethanol to ethylene [7]. These catalysts resulted in being selective to the dehydration reaction to ethylene, when mainly vanadium oxide monomeric species were present on a SBA-15 support [8].

Another important metal used for the dehydration of isopropanol is zirconium oxide, which increases the acidity of the reaction; however, it has not previously been set together with SBA-15 [9,10].

These promising results, together with the fact that isopropanol and ethanol have similar properties, have led us to examine the activity of V/Zr-SBA-15 catalysts in isopropanol dehydration. The SBA-15 materials included two different concentrations of zirconium in their structure and vanadium on their surface. We show that some of the tested catalysts appear to be suitable for the isopropanol dehydration reaction, achieving high activity in the conversion of isopropanol to propylene.

2. Results and Discussion

2.1. Characterization of the Catalysts

Zirconium-loaded zeolites, as well as the base materials studied in this work, are mesoporous solids. The goal of the catalysts' synthesis was to obtain zeolites containing 3% or 5% of zirconium and additionally 1% of vanadium. The results of the ICP analysis confirmed that the content of zirconium and vanadium in the samples was similar to those assumed during the synthesis of these catalysts. The compositions of the support and final catalysts are shown in Table 1.

Table 1. Chemical Zr and V (wt %) composition by ICP-OES of all the synthesized materials.

Catalyst	Assumed Chemical Composition (wt %)		Confirmed Chemical Composition (wt %)	
	Zr	V	Zr	V
SBA-15	0.00	0.00	0.00	0.00
Zr-SBA-15 I	3.00	0.00	2.95	0.00
Zr-SBA-15 II	5.00	0.00	5.49	0.00
1%V/Zr-SBA-15 I	3.00	1.00	2.81	0.88
1%V/Zr-SBA-15 II	5.00	1.00	5.02	0.80

The textural properties of all the solids were determined by mercury porosimetry and the specific surface area by nitrogen physisorption (Table 2). All materials were porous, having a large total intrusion volume and a high BET specific surface area (550–710 m² g⁻¹). The majority of the intrusion volume was attributable to macropores, typically 70% to 80% and a smaller proportion of 20% to 30% for mesopores of 3 to 50 nm.

Table 2. Textural properties of fresh support and catalysts.

Sample	Intrusion Volume (mL/g)		Median Pore Diameter (nm)	SBET (m ² /g)
	Total	Mesopores (3–50 nm)		
SBA-15	6.12	0.77	4.5	743.1
Zr-SBA-15 I	5.78	0.99	6.4	787.4
Zr-SBA-15 II	4.77	0.99	7.6	645.3
1%V/Zr-SBA-15 I	2.73	0.79	5.8	721.1
1%V/Zr-SBA-15 II	3.29	0.88	6.3	632.9

By introducing zircon into the structure, the mesopore volume increased by 30% and the median pore diameter increased from 4.5 to 6.4 nm for 3% of Zr and to 7.6 nm for the carrier with 5% of Zr (Table 2, Figure 1). This is the result of interactions occurring during the milling process that are used to produce catalysts, such as the dehydroxylation of zeolite, the reaction between external silanol groups and the zirconium salt precursor and ultimately the partial blocking of mesopores in zeolite by ZrO₂ particles.

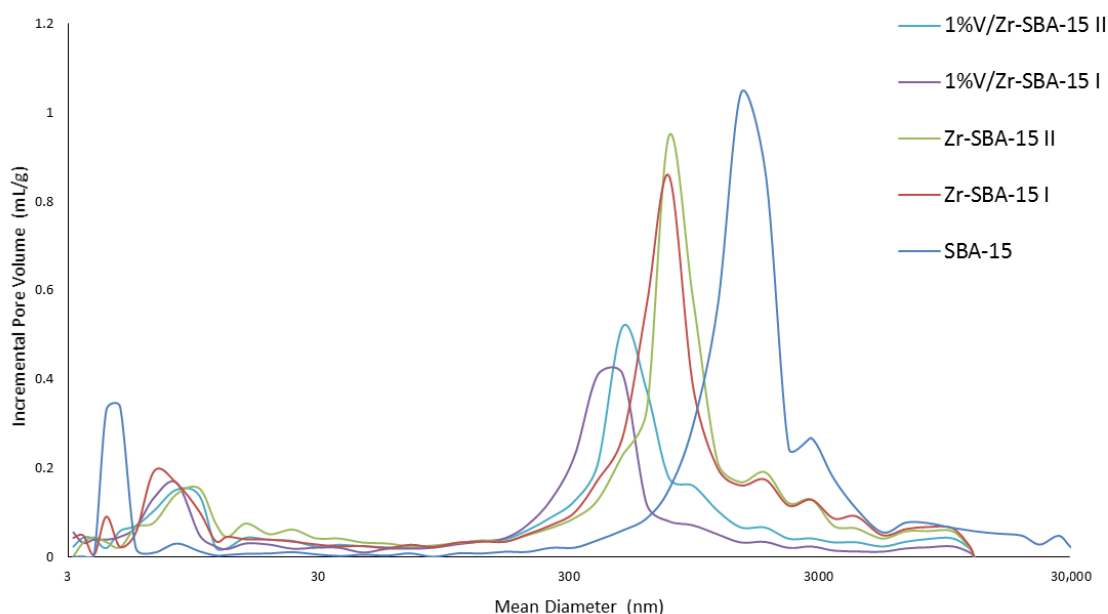


Figure 1. Mercury porosimetry analyses. Pore diameter and pore volume with a given diameter for the fresh catalysts.

In the case of adding vanadium by impregnation, the volume of pores, their diameter and the specific surface area of SBET decreased. The incorporation of Zr and V into the support reduces its surface area by approximately 30% (Table 2). We think that this is due to the formation of VO_x layers in the pores and surface of the support, as well as the formation of small fragments resulting from the impregnation and subsequent heat treatment of the catalysts. In addition, the volume and diameter of the mesopores decreased by 10% to 20% with impregnation; lower volumes were observed for the 1%V/Zr-SBA-15 II catalyst. The presence of macropores, along with a shorter length of mesoporous channels, improved the throughput of the reactants to active centers and the removal of products from the catalyst.

In the case of the used catalysts (Table 3), the results of the texture analysis showed that the surface area of the catalysts dropped by about 10% after tests.

Table 3. Textural properties of used supports and catalysts.

Sample	Intrusion Volume (mL/g)			Median Pore Diameter (nm)	SBET (m ² /g)
	Total	Mesopores (3–50 nm)	Macropores (50–12,000 nm)		
Zr-SBA-15 I	2.41	0.81	0.85	6.8	708.2
Zr-SBA-15 II	2.55	0.89	0.94	6.4	626.1
1%V/Zr-SBA-15 I	1.98	0.68	0.68	5.8	640.7
1%V/Zr-SBA-15 II	1.89	0.73	0.52	5.3	564.5

The mesoporous structure of the SBA-15 was confirmed by X-ray diffraction (XRD) at low angles along with scanning electron microscopy (SEM). The obtained diffractograms (Figure 2) showed characteristic diffraction lines (100), (110) and (200), which were less visible in vanadium catalysts.

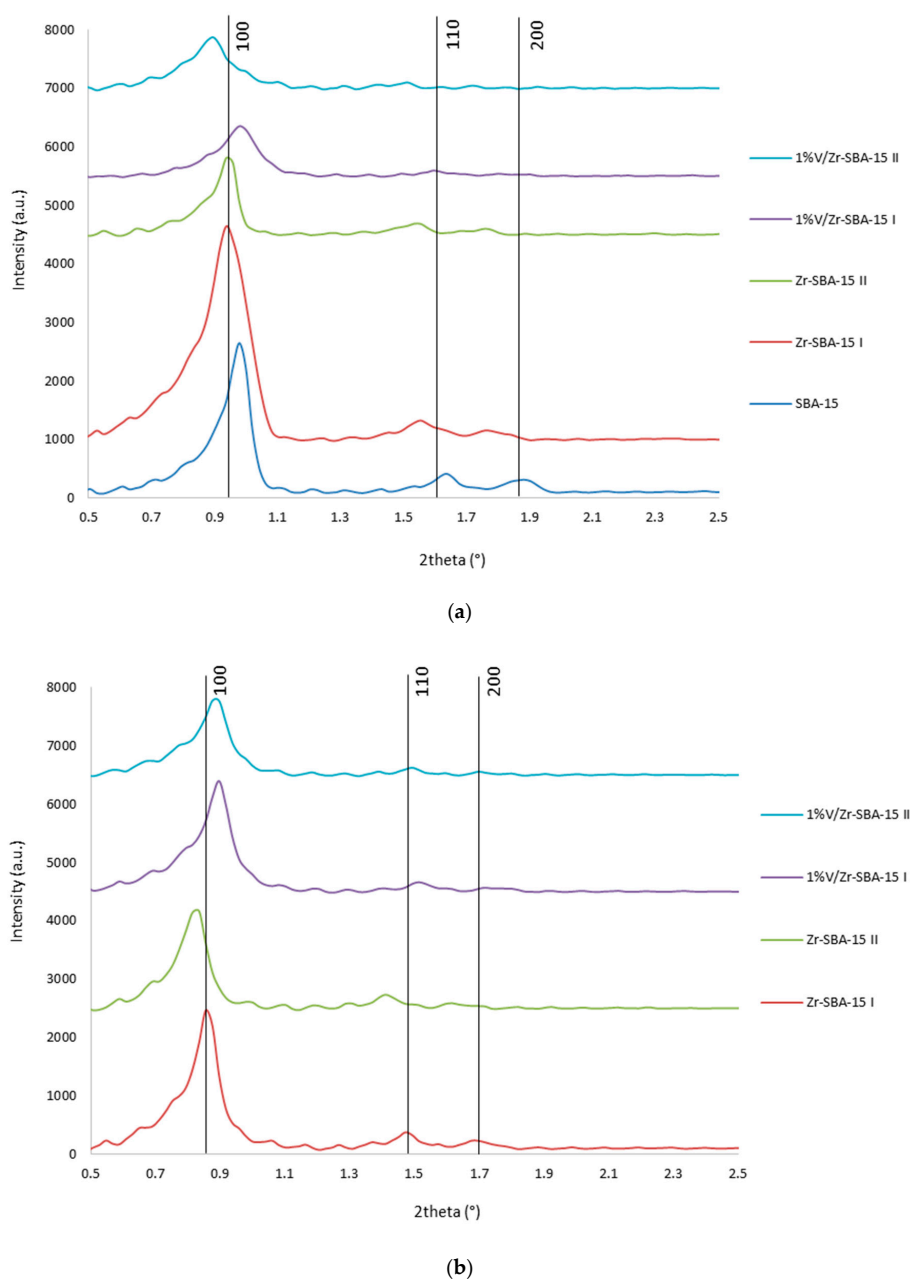


Figure 2. Small angle XRD diffraction pattern of Zr-SBA-15 supports and vanadium catalysts: fresh (a) and used (b).

The mesoporous SBA-15 structure in the vanadium catalysts was also confirmed by SEM. The SBA-15 and Zr-SBA-15 supports (Figure 3) showed a well-developed mesoporous structure very similar to the vanadium catalysts (Figure 4). The ordered SBA-15 structure with cylindrical hexagonal pores can be clearly distinguished in the SEM images of all samples. A greater share of small fragments produced during the impregnation and heat treatment of the catalysts was found. Embedding zircon into the structure caused the formation of particles of different thicknesses in the direction of the longitudinal axis of the pores. While the SBA-15 particles presented a thickness of 250–350 nm, Zr-SBA-15 I had a thickness of 150–200 nm and Zr-SBA-15 II was slightly thinner at about 130 nm. The shorter channel length was beneficial due to the diffusion of reactants into the pores and products from the pores, as measured in the resulting tests.

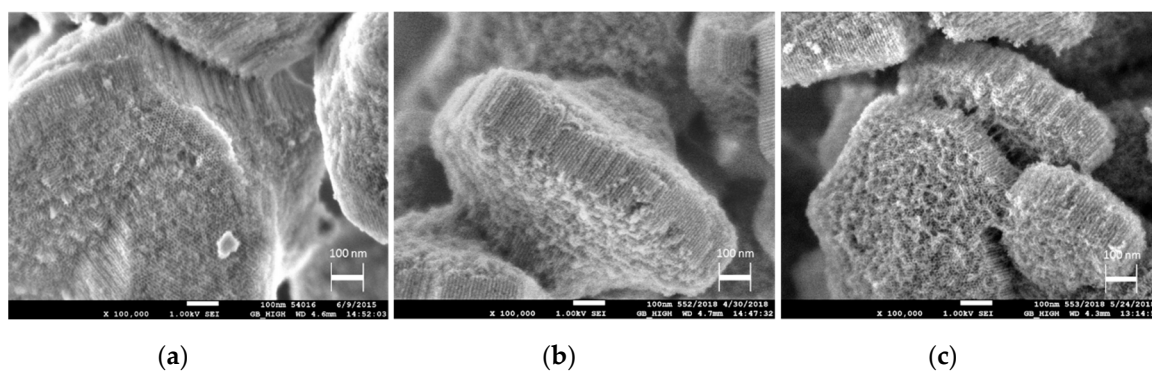


Figure 3. SEM images of SBA-15 (a), Zr-SBA-15 I (b) and Zr-SBA-15 II (c) catalysts (all images $\times 100,000$).

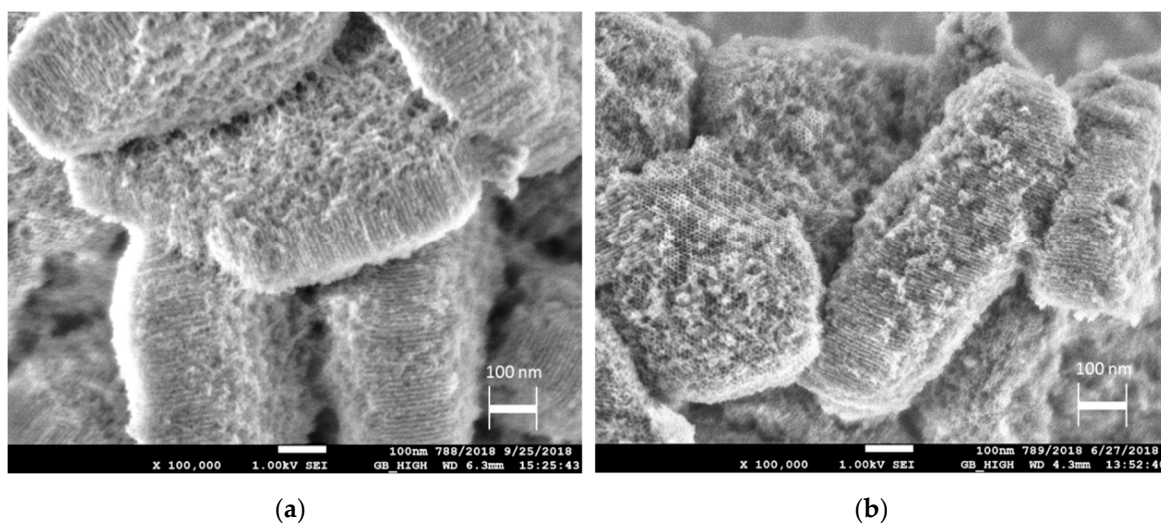


Figure 4. SEM images of 1%V/Zr-SBA-15 I (a) and 1%V/Zr-SBA-15 II (b) catalysts (all images $\times 100,000$).

The elemental analysis results suggest that the presence of carbon deposits in mesopores may be the cause of their decreasing volume. Mercury porosimetry showed a similar tendency (Figure 5), showing a decrease in the volume of the mesopores in the order of 10%–15%. However, XRD analysis was not able to show changes in the mesoporous structure of the used catalysts (Figure 2). The Raman spectroscopy also did not detect the carbon deposits, which should be visible as a characteristic band around 1580 cm^{-1} [11]. As the results of the elemental analysis show, the amount of carbon used in the catalysts is not large, typically about 1%. The used Zr-SBA-15 I and 1%V/Zr-SBA-15 I catalysts contained 1.08% and 1.12 wt % of carbon, respectively, while the Zr-SBA-15 II and V/Zr-SBA-15 II catalysts contained less carbon (0.66% and 0.83%, respectively). Carbon was present in lower amounts for catalysts with higher acidity.

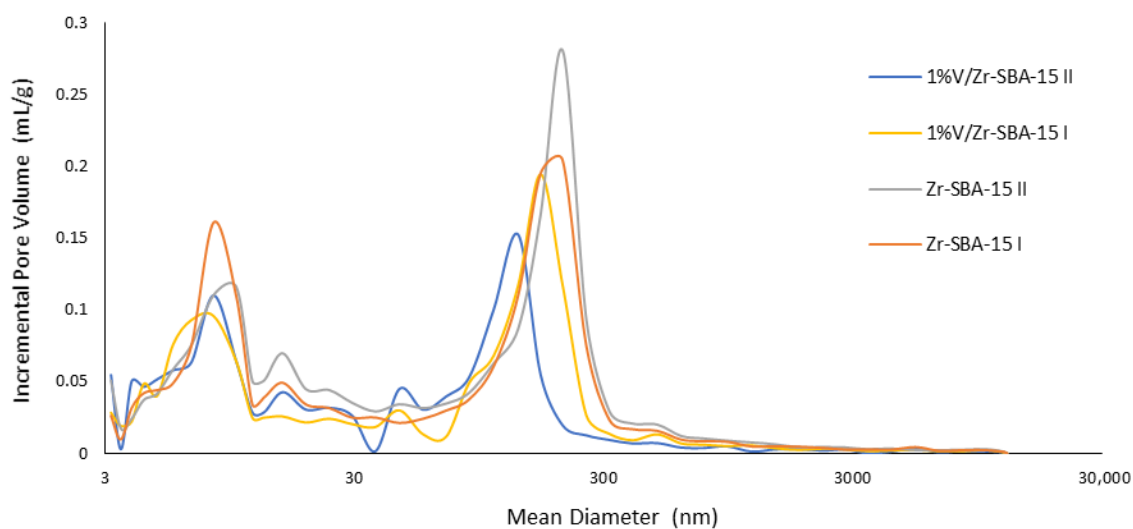


Figure 5. Mercury porosimetry analyses. Pore diameter and pore volume with a given diameter for the used catalysts.

The number of acidic centers and their strength, was determined by the temperature-programmable desorption of ammonia (NH_3 -TPD, Figure 6, Table 4). The SBA-15 solid contained mainly weak acidic centers. The addition of zirconium to the structure resulted in an increment in the number of strong acidic centers. This proportion increased with the increasing content of zirconium in the structure. Although the addition of vanadium caused an increase in active centers, it did not improve the catalyst activity toward propylene production. This is probably due to the redox VO_x activity proposed by Beck et al. [12].

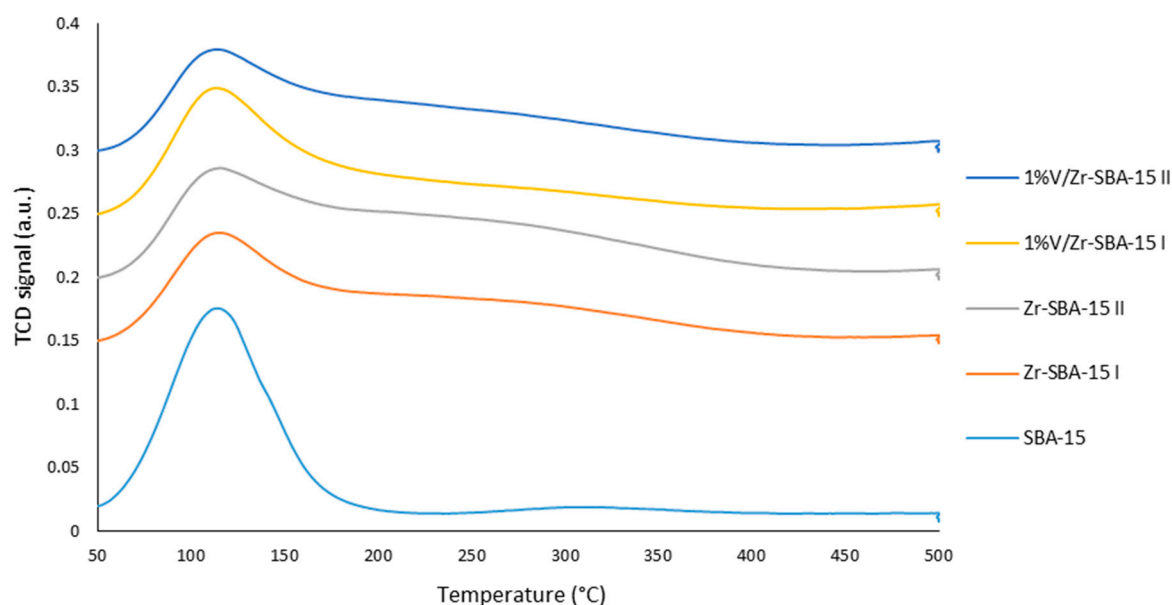
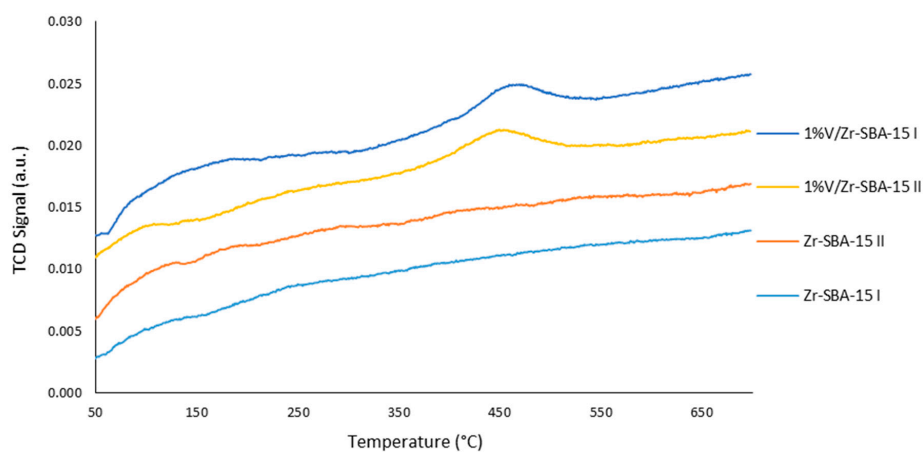


Figure 6. Temperature-programmable desorption of ammonia (NH_3 -TPD) profiles of catalysts.

Table 4. Properties of acid sites determined by NH₃-TPD. LT—low temperature sites; HT—high temperature sites.

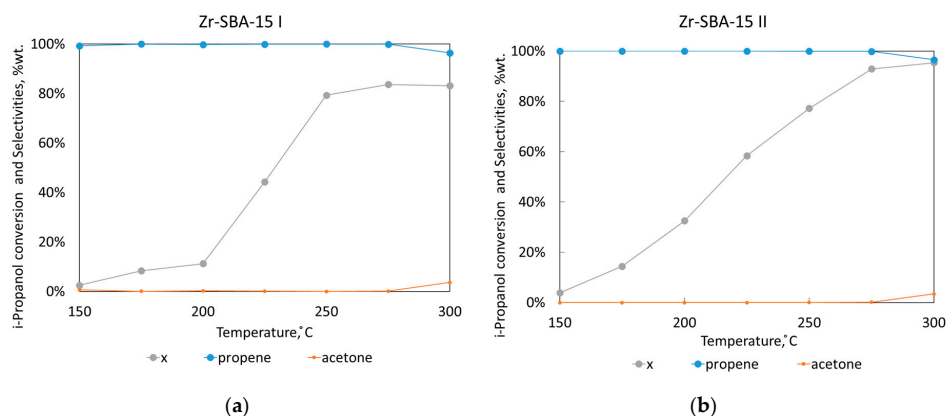
Sample	cSUM (μmol/g)	Tmax1 (°C)	cLT (μmol/g)	Population LT (%)	Tmax2 (°C)	cHT (μmol/g)	Population HT (%)
SBA-15	1169	114	1118	95.6	311	52	4.4
Zr-SBA-15 I	1051	113	608	57.8	220	443	42.2
Zr-SBA-15 II	1092	112	509	46.6	227	584	53.4
1%V/Zr-SBA-15 I	1148	113	521	45.4	242	627	54.6
1%V/Zr-SBA-15 II	1408	114	625	44.4	247	784	55.6

Due to the low content of vanadium in the catalysts, the changes in the temperature-programmed reduction (Figure 7) were not significant between the two vanadium catalysts. There was only a slight shift of the reduction peak at 462 °C for the V/Zr-SBA-15 I catalyst and at 470 °C for the V/Zr-SBA-15 II catalyst.

**Figure 7.** H₂-TPR patterns for all catalysts.

2.2. Catalytic Tests

For all catalytic tests, the conversion of isopropanol increased with increasing temperature. Three samples were taken at each temperature, at an hourly interval, for analysis with gaseous chromatography and their results were almost the same. A high increment in the conversion was found in all catalysts in the range of 200–250 °C (Figures 8 and 9).

**Figure 8.** Isopropanol conversion and selectivity to propene and acetone for the Zr-SBA-15 I (a) and Zr-SBA-15 II (b) catalysts.

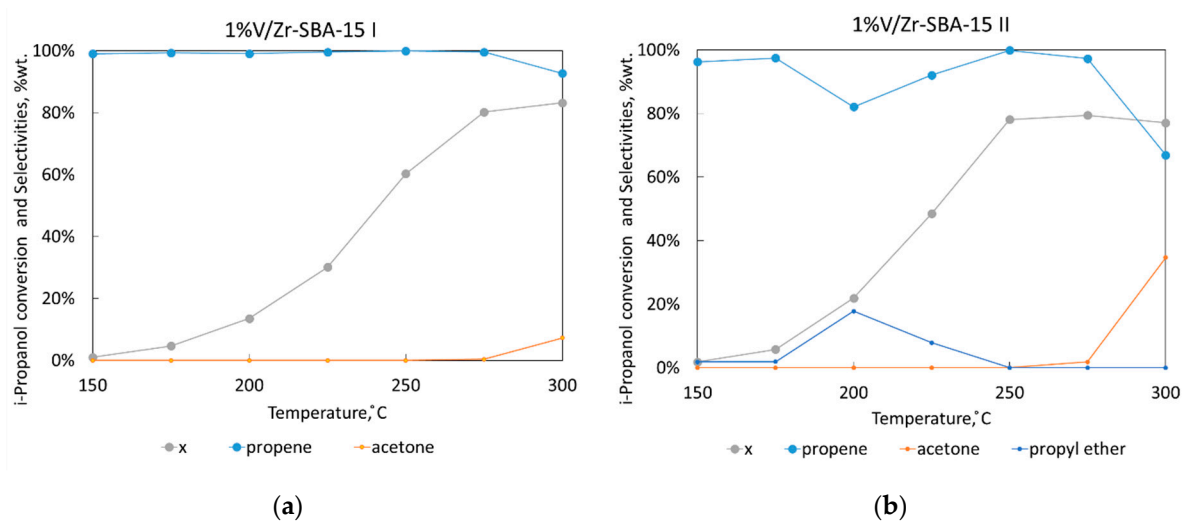


Figure 9. Isopropanol conversion and selectivity to propene and acetone for the 1%V/Zr-SBA-15 I (a) and 1%V/Zr-SBA-15 II (b) catalysts.

The exception was SBA-15, for which the conversion was very low and reached only 5.65% at the highest point. In the case of the Zr-SBA-15 II material, the conversion was 96 wt %. The main reaction product was propylene. Despite a variable conversion initially, the selectivity to propylene was almost maintained at 100 wt %. The highest selectivity was noted for the reaction catalyzed by Zr-SBA-15 I and Zr-SBA-15 II.

However, the use of vanadium supported on the Zr-SBA-15 materials resulted in an increase in the production of side product (acetone and propyl ether). The lowest conversions, selectivity and the largest amount of side products were observed in the 1%V/Zr-SBA-15 II catalyzed reaction.

The reaction achieved a total conversion of 96% with a selectivity to propylene of 100%. Similar results were presented by Bedia et al., obtaining a conversion of 95% at full selectivity to propylene, also at 275 °C [13]. However, in his research he used strong H_3PO_4 acid and used 11,000 times lower WHSV ($0.001\ h^{-1}$), which reduces the amount of product obtained and reduces the industrial utility of this path of propylene synthesis. In turn, Larmier et al. decided to lower the temperature and increase WHSV to $2.8\ h^{-1}$, which resulted in an increased conversion (40%) while maintaining 100% selectivity [14]. In research conducted on $\gamma-Al_2O_3$ catalysts, they focused mainly on studying the thermodynamics of the reaction and concluded that the key effect on selectivity is temperature, while catalytic activity is determined by the morphology of the catalyst. This was partly confirmed in our research, as we also noticed the influence of catalyst geometry on the availability of active centers; however, regardless of the catalyst, the conversion also increased with increasing temperature. Foo et al. increased the temperature range (286–320 °C) and WHSV ($0.95\ h^{-1}$); using perovskite catalysts, the substrate was mostly dehydrogenated, over dehydrated and as a result the main reaction product was acetone [9]. Although Blanco-Bonilla et al. obtained a high selectivity (92%) for a higher WHSV ($23.6\ h^{-1}$), it resulted in poor conversion (15%) [10]. For the first time, Zr-SBA-15 materials were tested in isopropanol dehydration, resulting in the highest conversion found that we are aware of in the literature of heterogeneous catalysis. In addition, due to the use of a much bigger stainless-steel reactor, one gram of catalyst was used compared to the few milligrams used by other authors and a potential industrial application was found.

3. Materials and Methods

3.1. Preparation of the Catalysts

SBA-15 mesoporous material was synthesized according to the method described by Zukal et al. [11]. Amphiphilic triblock copolymer Pluronic[®] P123 (Sigma-Aldrich, Schnellendorf,

Germany), which served as a structure model, was immersed in the acidic reaction medium obtained using an aqueous solution of hydrochloric acid (35% by weight, Lach-Ner s.r.o., Neratovice, Czech Republic). Silica was provided by the addition of tetraethyl orthosilicate (TEOS, Sigma-Aldrich, Schnelldorf, Germany). A reaction mixture with a molar ratio of 1 TEOS:0.017 P123:6.1 HCl:197 H₂O was prepared at 35 °C and after 24 h heated at 95 °C for 66 h under static conditions. The product was obtained by filtration, washing with distilled water and drying at 80 °C overnight. To remove the template, the calcination was carried out in air at 540 °C for 8 h (ramp temperature 1 °C min⁻¹). The SBA-15 was enhanced by supplementation with zirconia (Zr-SBA-15) or with zirconia and vanadium (1%V/Zr-SBA-15). The zirconia catalysts were prepared in two variants, varying by the percentage of the added zirconia enrichment (ZrOCl₂, Lach-Ner). The zirconium was added in the appropriate amount for obtaining two catalysts containing 3 wt % and 6 wt % of zirconium, respectively, using the method developed by Zukal et al. [15]. To obtain the vanadium catalysts, the support was impregnated with aqueous solution with a molar ratio of 1 H₂O₂:4 H₂O and the appropriate amount of ammonium metavanadate (Sigma-Aldrich, Schnelldorf, Germany) for a final catalyst containing 1 wt % of vanadium. The final products were obtained by drying overnight in a stream of air at 120 °C and calcined in air flow at 450 °C for 6 h. Five catalysts were synthesized, one pure SBA-15 solid, two Zr-SBA-15 named Zr-SBA-15 I (3 wt % of Zr) and Zr-SBA-15 II (5 wt % of Zr) and two V(1 wt %)/Zr-SBA-15 named 1%V/Zr-SBA-15 I and 1%V/Zr-SBA-15 II, which contained the Zr-SBA-15 I and Zr-SBA-15 II supports, respectively.

3.2. Characterization of the Catalysts

The composition of the catalysts was verified by using an ICP-OES Agilent 725 (Agilent Technologies Inc., Santa Clara, USA). Before analysis, 500 mg of the sample was dissolved in 10 mL of H₂SO₄ (1:1). The undissolved residue from acid leaching was filtered with a paper filter, burned and silicon oxide was removed by HF. Residues from HF leaching were melted with KHSO₄, dissolved in water and added to filtrate. Finally, the sample solution was introduced into a volumetric flask and measured.

XRD was used to determine the crystallographic structure of the catalysts. The samples were analyzed using a D8 Advance Eco (Bruker, Billerica, USA), applying Cu K α radiation ($\lambda = 1.5406 \text{ \AA}$), 0.5 s step time and 0.02° step size. Data collected in the 2 θ range from 0.5° to 70° were analyzed using Diffrac.Eva V 4.1.1 (Bruker, Billerica, USA) software with the Powder Diffraction File database (PDF 4 + 2018, International Centre for Diffraction Data).

To assess the morphology of the catalysts, a scanning electron microscope (JEOL JSM-7500F) with cold emission to the cathode field at 1 kV in GB high mode was used.

The specific surface area (BET) of the solids was determined using N₂ adsorption/desorption at -196 °C with an Autosorb iQ (Quantachrome Instruments, Boynton Beach, USA). The solids were dried before each analysis in a glass cell at 200 °C under vacuum for 16 h. Mercury porosimetry measurements were performed on a Micromeritics AutoPore IV 9510. All samples were dried before the analysis in a glass cell at 200 °C (under vacuum for 16 h).

NH₃ temperature-programmed desorption (TPD) was used to characterize the acid-base properties of the catalysts. An Autochem 2950 HP (Micromeritics Instrument Corporation, Norcross, USA) was used. For each analysis, 100 mg of sample was pretreated in He to 500 °C (10 °C min⁻¹). In this case, the sample was cooled to 50 °C before being saturated with ammonia (25 mL min⁻¹ of 10 vol% NH₃/He for 30 min). Then, helium was used (25 mL min⁻¹) to remove physically/weakly adsorbed ammonia with a constant baseline (60 min). After that, the temperature was increased to 500 °C (15 °C min⁻¹). The NH₃ concentration was monitored using a TCD detector.

The vanadium species reducibility was determined by H₂-TPR (AutoChem 2950 HP, Micromeritics Instrument Corporation, Norcross, USA). A total of 100 mg of the sample (50 mg for V/Zr-SBA-15) was treated in oxygen flow (300 °C (2 h)) before measurement. The reduction test was performed

at 40–700 °C (10 °C min⁻¹) under hydrogen (5 vol % H₂ in Ar). The hydrogen concentration was monitored using a TCD detector.

The carbon content was determined by elemental analysis of the solid powder using a Flash2000 (Thermo Fisher Scientific, Waltham, USA). The sample (2.5 mg) was mixed with oxidant (V₂O₅) and burned in oxygen flow at 950 °C. The resulting gas was reduced to CO, separated with a chromatic column and detected by the TCD detector. The measurement was performed three times to assure its repeatability.

The carbon content was also determined by Raman spectral analysis. For this analysis, a DXR-Smart Raman (Thermo Fisher Scientific, Waltham, USA) with an intelligent exciting laser (Thermo Fisher Scientific, Waltham, USA) was used, using a laser wavelength of 780 nm. Powdered samples were thermally activated in a vacuum and placed in a Pyrex cuvette. Spectra analysis was performed at a resolution of 2 cm⁻¹; 400 scans were made for each sample and for each scan, the integration time was 5 s.

3.3. Catalytic Tests

A continuous flow reactor with a set of ten thermocouples in the catalytic bed was used. The inner diameter of the reactor was 17 mm. The net diameter of the catalyst bed was 10.7 mm and the total volume was 60 mL. A minimal amount of quartz wool was placed at the bottom of the reactor. Then, a mixture (60 mL) of catalyst (1 g) and SiC (enough to fill the 60 mL of the total final volume) were introduced into the reactor. The catalyst was activated at 300 °C under nitrogen atmosphere (50 NL h⁻¹) for 2 h. The reaction was carried out with a total helium gas flow rate of 50 NL h⁻¹ and an isopropanol feed flow rate of 11 g h⁻¹. Under these conditions, the reaction was performed at different temperatures (150, 175, 200, 225, 250, 275 and 300 °C). At each temperature, the test was performed for 3 h and three samples were obtained (each one after 1 h). A sampling system of the reactor consisted of two collectors. A liquid product was cooled by water at room temperature (20 °C) in the first collector and at 0 °C in the second collector. Liquid samples were immediately analyzed by gas chromatograph (GC) in the laboratory. An online GC-FID equipped with a HP-Pona column (50 m × 0.25 mm, He as the carrier gas) was used. The general conditions in the GC were the same as those used for ASTM D6730 for a GC, with the oven temperature being maintained at 100 °C for the duration of the analysis and the products of the isopropanol dehydration being measured instead of gasoline (ASTM D6730 is orientated to gasoline analyses). In addition, after the second collector, the gaseous flow was collected and analyzed by GC (Refinery Gas Analysis (RGA), Agilent Technologies Inc., Santa Clara, USA). Calibration was carried out for the quantitative analyses.

4. Conclusions

Four zeolite-based catalysts were synthesized in this work. Catalysts were prepared by incorporating 3% or 5% by weight of zirconium and 1% by weight of vanadium into the structure of SBA-15. The materials were then characterized by ICP, SEM, XRD, Hg porosimeters, SBET, TPD and TPR. The incorporation of Zr nanoparticles (in the form of ZrO₂) leads to a decrease in the specific surface area of the catalyst, changes its geometry and affects the acidic center distribution.

This study provides evidence that the addition of vanadium on the SBA-15 surface or zirconium to the mesoporous SBA-15 structure changes the geometry of the catalyst, affecting the acidic center distribution, which in turn has an influence on the catalyst's activity. The catalyst without vanadium but with added zirconium (Zr-SBA-15 II) proved to be an effective material for the dehydration of isopropanol, showing the best results in comparison to existing studies and ensuring a selectivity to propylene of 100% at 96% conversion.

Author Contributions: Conceptualization, M.M., Z.T., J.Š. and J.M.H.-H.; methodology, M.M. and Z.T.; software, J.Š.; validation, M.M., Z.T., J.Š. and J.M.H.-H.; formal analysis, M.M., Z.T., J.Š. and J.M.H.-H.; investigation, M.M. and Z.T.; resources, M.M., Z.T., J.Š. and J.M.H.-H.; data curation, M.M., Z.T., J.Š. and J.M.H.-H.; writing—original draft preparation, M.M. and Z.T.; writing—review and editing, J.Š. and J.M.H.-H.; visualization, M.M. and Z.T.;

supervision, J.M.H.-H.; project administration, J.Š.; funding acquisition, J.Š. All authors have read and agreed to the published version of the manuscript.

Funding: This publication is a result of the Development of the UniCRE Centre project (LO1606), which has been financially supported by the Ministry of Education, Youth and Sports of the Czech Republic (MEYS) under the National Sustainability Program I. The result was achieved using the infrastructure of the Efficient Use of Energy Resources Using Catalytic Processes project (LM2015039), which has been financially supported by MEYS within the targeted support of large infrastructures.

Conflicts of Interest: The authors declare no conflict of interest. The funders had no role in the design of the study; in the collection, analyses or interpretation of data; in the writing of the manuscript; or in the decision to publish the results.

References

1. Al-Douri, A.; Sengupta, D.; El-Halwagi, M.M. Shale gas monetization—A review of downstream processing to chemicals and fuels. *J. Nat. Gas Sci. Eng.* **2017**, *45*, 436–455. [[CrossRef](#)]
2. Corma, A.; Corresa, E.; Mathieu, Y.; Sauvanaud, L.; Al-Bogami, S.; Al-Ghrami, M.S.; Bourane, A. Crude oil to chemicals: Light olefins from crude oil. *Catal. Sci. Technol.* **2017**, *7*, 12–46. [[CrossRef](#)]
3. Akah, A.; Al-Ghrami, M. Maximizing propylene production via FCC technology. *Appl. Petrochem. Res.* **2015**, *5*, 377–392. [[CrossRef](#)]
4. Walther, T.; François, J.M. Microbial production of propanol. *Biotechnol. Adv.* **2016**, *34*, 984–996. [[CrossRef](#)] [[PubMed](#)]
5. Frank, B.; Dinse, A.; Ovsitser, O.; Kondratenko, E.V.; Schomäcker, R. Mass and heat transfer effects on the oxidative dehydrogenation of propane (ODP) over a low loaded VO_x/Al₂O₃ catalyst. *Appl. Catal. A Gen.* **2007**, *323*, 66–76. [[CrossRef](#)]
6. Chokkalingam, S.; Viswanathan, B.; Varadarajan, T.K. Decomposition of isopropyl alcohol on g-phase bismuth molybdate catalyst. *Indian J. Chem.* **1984**, *23*, 143–144.
7. Čičmanec, P.; Raabová, K.; Hidalgo, J.M.; Kubička, D.; Bulánek, R. Conversion of ethanol to acetaldehyde over VO_x-SiO₂ catalysts: The effects of support texture and vanadium speciation. *React. Kinet. Mech. Catal.* **2017**, *121*, 353–369. [[CrossRef](#)]
8. Čičmanec, P.; Ganjkanlou, Y.; Kotera, J.; Hidalgo, J.M.; Tišler, Z.; Bulánek, R. The effect of vanadium content and speciation on the activity of VO_x/ZrO₂ catalysts in the conversion of ethanol to acetaldehyde. *Appl. Catal. A Gen.* **2018**, *564*, 208–217. [[CrossRef](#)]
9. Foo, G.S.; Polo-Garzon, F.; Fung, V.; Jiang, D.; Overbury, S.H.; Wu, Z. Acid–base reactivity of perovskite catalysts probed via conversion of 2-propanol over titanates and zirconates. *ACS Catal.* **2017**, *7*, 4423–4434. [[CrossRef](#)]
10. Blanco-Bonilla, F.; Lopez-Pedrajas, S.; Luna, D.; Marinas, J.M.; Bautista, F.M. Vanadium oxides supported on amorphous aluminum phosphate: Structural and chemical characterization and catalytic performance in the 2-propanol reaction. *J. Mol. Catal. A Chem.* **2016**, *416*, 105–116. [[CrossRef](#)]
11. Zukal, A.; Siklová, H.; Cejka, J. Grafting of alumina on SBA-15: Effect of surface roughness. *Lagmuir* **2008**, *24*, 9837–9842. [[CrossRef](#)] [[PubMed](#)]
12. Beck, B.; Harth, M.; Hamilton, N.G.; Carrero, C.; Uhlrich, J.J.; Trunschke, A.; Shaikhutdinov, S.; Schubert, H.; Freund, H.J.; Schlögl, R.; et al. Partial oxidation of ethanol on vanadia catalysts on supporting oxides with different redox properties compared to propane. *J. Catal.* **2012**, *296*, 120–131. [[CrossRef](#)]
13. Bedia, J.; Ruiz-Rosas, R.; Rodríguez-Mirasol, J.; Cordero, T. A kinetic study of 2-propanol dehydration on carbon acid catalysts. *J. Catal.* **2010**, *271*, 33–42. [[CrossRef](#)]
14. Larmier, K.; Chizallet, C.; Cadran, N.; Maury, S.; Abboud, J.; Lamic-Humblot, A.F.; Marceau, E.; Lauron-Pernot, H. Mechanistic investigation of isopropanol conversion on alumina catalysts: Location of active sites for Alkene/Ether production. *ACS Catal.* **2015**, *5*, 4423–4437. [[CrossRef](#)]
15. Zukal, A.; Pastva, J.; Čejka, J. MgO-modified mesoporous silicas impregnated by potassium carbonate for carbon dioxide adsorption. *Microporous Mesoporous Mater.* **2013**, *167*, 44–50. [[CrossRef](#)]

